

Research Article

Condition-Based Monitoring on High-Precision Gearbox for Robotic Applications

Mohamad Amin Al Hajj ¹, Giuseppe Quaglia ², and Ingo Schulz ³

¹Politecnico di Torino, Turin 10129, Italy

²Department of Mechanical and Aerospace Engineering, Politecnico di Torino, Turin 10129, Italy

³SKF GmbH, Schweinfurt 97421, Germany

Correspondence should be addressed to Mohamad Amin Al Hajj; aminalhajj.mohamad@gmail.com

Received 29 November 2020; Revised 28 March 2022; Accepted 31 March 2022; Published 25 April 2022

Academic Editor: Yi Qin

Copyright © 2022 Mohamad Amin Al Hajj et al. This is an open access article distributed under the Creative Commons Attribution License, which permits unrestricted use, distribution, and reproduction in any medium, provided the original work is properly cited.

This work presents a theoretical and experimental study regarding defect detection in a robotic gearbox using vibration signals in both cyclostationary and noncyclostationary conditions. The existing work focuses on inferring the health of the robot during operation with little regard toward the defective element of the components. This article illustrates the detection of specific element damage of a robotic gearbox during a robotic cycle based on domain knowledge and presents a novel data-driven method for asset health. This starts by studying the robotic gearbox, specifically its kinematics as a planetary 2-stage reduction gearbox to acquire the knowledge of the rotations of each component. The signals acquired from a test bench with four sensors undergo different acquisition methods and signal processing techniques to correlate the elements' frequencies. The work shows the detection of the artificially created defects from the acquired vibration data, verifying the kinematic methodology and identifying the root cause of failure of such gearboxes. A novel resampling method, Binning, is presented and compared with the traditional signal processing techniques. Binning combined with Principal Component Analysis (PCA) as a data-driven method to infer the state of the gearbox is presented, tested, and validated. This work presents methods as a step toward automatized predictive maintenance on robots in industrial applications.

1. Introduction

The prediction of failure in machines has attracted interest in the research community targeting shorter downtime, higher reliability, and lower maintenance cost [1]. This presented instruments, such as sensors and computational devices, in addition to numerous methodologies to unearth the root cause of failure in machines [2]. With the developments seen in manufacturing, advanced manufacturing systems became more complex [3] in conjunction with the rise of robots' density worldwide [4]. The installations of industrial robots increased by 6% to 422,271 in 2019 worth USD 16.5 billion with a forecast of +12% per year from 2020 to 2022 [5]. Robots causing 20% of downtime in highly automated lines [6] make their health and their components worthy asset to be studied.

Kim et al. [7] proposed a phase-based time domain averaging method to detect faults in gearboxes of industrial robots. The method used vibration signals to detect the failure of the gearbox and not specific elements barring the need of constant angular speed conditions, which may not be present in some industrial robotic cycles. Khalastchi et al. [8] developed a hybrid, unsupervised online and supervised offline, to improve fault detection in robotic systems. The technique showed better results than the unsupervised method in most cases but did not reveal the cause of failure and needs enhancements as the authors suggest. Wing K. To et al. [9] presented an approach to fault diagnosis using three sensing modalities during a robotic operation. The work showed over 95% accuracy but was limited to a singular operation within a laboratory environment. Costa et al. [10] demonstrated classification models in industrial robotic

arms, using machine learning and statistical methods, to detect failure. The article showed various methods performing differently for different joints with the writers recommending more data to improve the statistical methods. Mien et al. [11] investigated an algorithm for robust fault diagnosis in robotic systems in the presence of modelling uncertainties. The proposed method was demonstrated to show effectiveness in computer simulations of 3-degree-of-freedom robot. The research mentioned focuses on faults of a robot; however, present are investigations on the components, specifically the power transmission in robotics. Schempf and Yoerger [12] studied the performance differences between various robots' transmissions. Their work showed how task performance requirements impact the transmission selection through data and analytical techniques. Although the mentioned publication explores the robot as a monitored asset, work has been done on high-reduction gearboxes and systems.

The health of high-reduction ratio gearboxes, a component of the power transmission system, was a subject of investigations. Chang et al. [13] proposed a one-dimensional fully decoupled network for planetary gearboxes health status identification. The method acquired vibration signals from the gearbox setup to then apply the suggested algorithm with limitations especially with the determination of the algorithm's parameters. Barbieri et al. [14] identified the presence of damage and diagnosed the component by comparing vibration signals of damaged and undamaged systems. The faults were directly verified by the contrast of energy levels and entropy of the two systems. Interesting research done by Plöger et al. [15] where the experimental data correlates partially with the existing research related to vibration signals and planetary gearboxes. The experiment included testing six commodity gearboxes where vibration data could only be partially explained due to the noticeable deviations from the mathematical models.

Research work in fault detection is also present in the field of gearbox elements as in gears and bearings using vibration signals. Several articles [16–21] study the possibility of detecting damages of gears with vibration data. Bearings are also present in gearboxes and researches published various articles on detecting their defects during operation [22–26].

The work to be presented in this article is towards the identification of faults inside a complex cycloidal gearbox consisting of both bearings and gears in normal robotic operating conditions. Regarding the previously mentioned work, the detection of the root cause of failure was absent with a focus on the gearbox being faulty or not in robotic cycles in industrial applications. Although the presence of several components emitting vibration signals is challenging, the methodology described in this article can reveal the present defects. The identification is based on a kinematic study of each element of the gearbox to infer their specific operating cycles allowing the knowledge of their respective faulty frequencies. These are then correlated with the acquired and processed vibration data from the four mounted sensors on the test rig. The observation of the elements' defect frequencies corresponds to the detection of damage

on that specific entity of a robot in industrial applications. Another method using a novel method, Binning, and a machine learning technique, PCA, is evaluated to detect faults within the gearbox.

The contribution of this paper is as follows: a purely data-driven method to detect defects using the Binning algorithm and PCA in both cyclostationary and noncyclostationary conditions. The method proposed removes the need of an additional sensor, the tachometer, as the robotic cycle motion and the vibration signals are correlated. This method is compared to traditional methods in terms of frequency demonstrations. The kinematic study of this high-precision gearbox combined with traditional approach allows the identification of the defect component before failure.

The structure of this research starts in Section 2 where the cycloidal gearbox, the Nabtesco RV-42N, and its characteristics are shown as well as the test rig, its components, and the sensors positioning relative to the gearbox. The state of the gearbox being monitored with its faults is also shown. Section 3 demonstrates the kinematic study of the gearbox along with the signal processing techniques to be used for cyclostationary and noncyclostationary conditions. This section also provides the expected emitted frequencies of the vibration signals in the presence of a damaged component and presents the Binning algorithm with PCA. Section 4 describes the acquired signals, analysis, and discussion moving into the conclusion, which is found in Section 5.

2. The Gearbox, Its State, and the Test Rig

In this section, the chosen gearbox is described with its elements from the gears to the bearings and its operating principle. The state of the gearbox is discussed, that is, the damage inflicted to it and the overall health of its components. In the final part of this section, the test rig implementation is illustrated from the operating cycle to the sensors and signal acquisition kit.

2.1. Nabtesco RV-42N. Knowing that Nabtesco's RV series gearboxes have a high share of the global market for industrial robot joints [27], the adopted gearbox is the Nabtesco RV-42N. Figure 1, courtesy of Nabtesco, presents the mechanical structure of the gearbox with indications of its elements that achieve a high reduction ratio. In the figure, s refers to the excentre present and s' to the overall output carrier.

It consists of 2-stage reduction where the first is a spur gear reduction stage from the input pinion that is fixed onto the motor. The second is a hypocycloidal reduction stage that transfers the speed and the amplified torque to the output side. The epicyclic gears are offset 180° from one another to provide a balanced load and negate vibration generation. In addition to the components mentioned, more are present as bearings which aid the rotational motion of the gearbox.

The Nabtesco RV-42N is a hypocycloidal gearbox with 3 input spur gears and 2 cycloidal disks rotating around pins. The nomenclature of the components will be Nabtesco's as

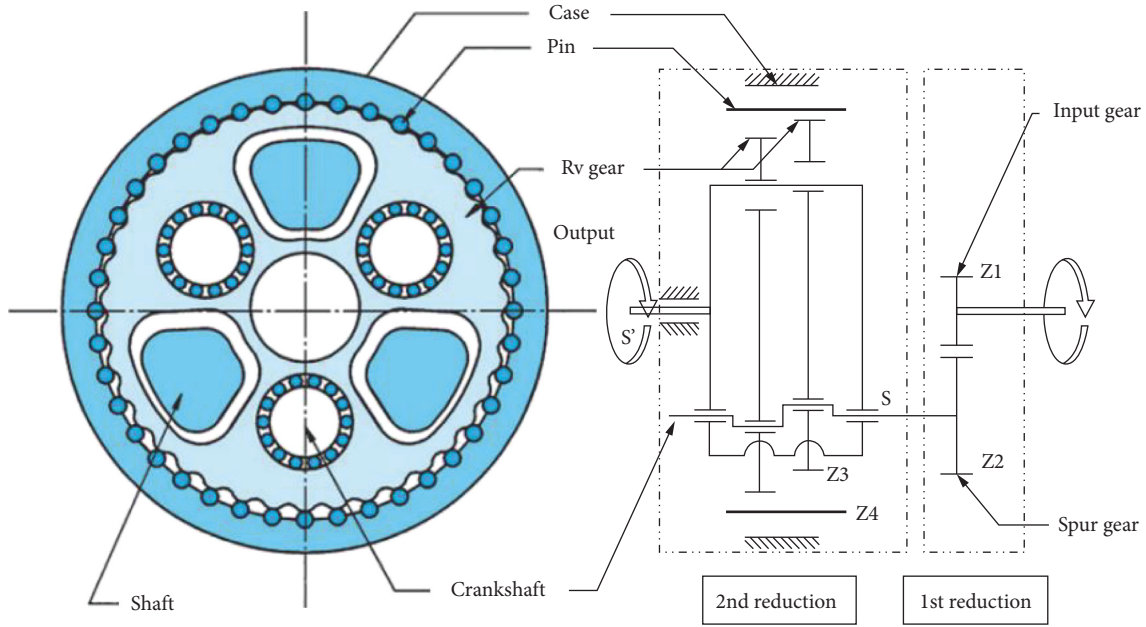


FIGURE 1: Nabtesco's RVN mechanism block [27].

reported in Figure 1 in addition to the present bearings termed Angular Contact Ball Bearing (ACBB), Cylindrical Roller Bearing (CRB), and Tapered Roller Bearing (TRB). Table 1 reports the number of elements found in this gearbox.

2.2. The Gearbox's Condition. In its initial form, the gearbox is defect free and it is tested to acquire some firsthand knowledge regarding the emission of vibration signals. The Nabtesco RV-42N is shown in Figure 2 where it is dismantled, and all its elements are visible. Instead of running until failure and the scope being condition based monitoring, the decision to make artificial damages was made.

Considering that failure of gearboxes is related 70% of the time to bearing damages and 26% to gears [28], both are chosen to be damaged. Due to the complexity to dismantle the internal components, some elements of the components were not easily reachable, such as the rollers of the TRBs. The artificial damages were made with a milling tool and the damages were chosen to be on 3 elements: the ACBB's outer ring, the CRB's outer ring, and the RV gear's undulations that could represent surface spalling. The size of the damages was not quantified, but was visually considered to be sufficient to check if defects can be detected.

The damages depicted in Figure 3 correspond to specific frequencies separate from each other so that they can be easily identifiable. The damages reported are in order from left to right as follows: ACBB's outer ring, CRB's outer ring, and disk undulation damage. These are well known and reported in the kinematic study in Section 3.

2.3. Test Rig. This section provides the necessary information regarding the test rig and sensors setup. Figure 4 depicts the tools that are connected to the test rig where the gearbox

TABLE 1: Nabtesco RV-42N components.

Element	Count (total number)
Input gear	1
Spur gear	3
RV gear	2
ACBBs	2
CRBs	6
TRBs	6
Input gear teeth (Z1)	16
Spur gear teeth (Z2)	50
RV gear undulations (Z3)	39
Internal pins (Z4)	40

setup is present. It contains the signal acquisition kit in direct connection to the sensors through cable connections. The kit includes the condition monitoring system from SKF connected to SKF's sensor on the rig and managing the data transfer to the computer. The computer is installed to allow the visualization and storage of the acquired signals. The control panel is used for the correct operation of the gearbox setup along with the emergency stop button. Both are located outside the cage where the actual setup is placed.

Figure 4 describes the components found outside the safety cage and Figure 5 illustrates the sensor placement for the signal acquisitions. As shown, there are 5 medium sensitivity, 100 mV/g, accelerometers of which 4 are used for vibration data acquisition and 1 is used as an emergency stop in case the vibration signals exceed the predefined limits. On the other side, there is the tachometer used to acquire the variations of rotational velocity at the input side. Table 2 presents the sensors used in addition to the gearbox setup's parameters that Figure 5 describes.

The positioning of the 4 vibration sensors, Acc1, Acc2, Acc3, and Acc4, is done to acquire vibration signals in all three directions with Acc0, the sensor responsible for the



FIGURE 2: Dismantled nabtesco RV-42N.



FIGURE 3: Gearbox artificial damages.

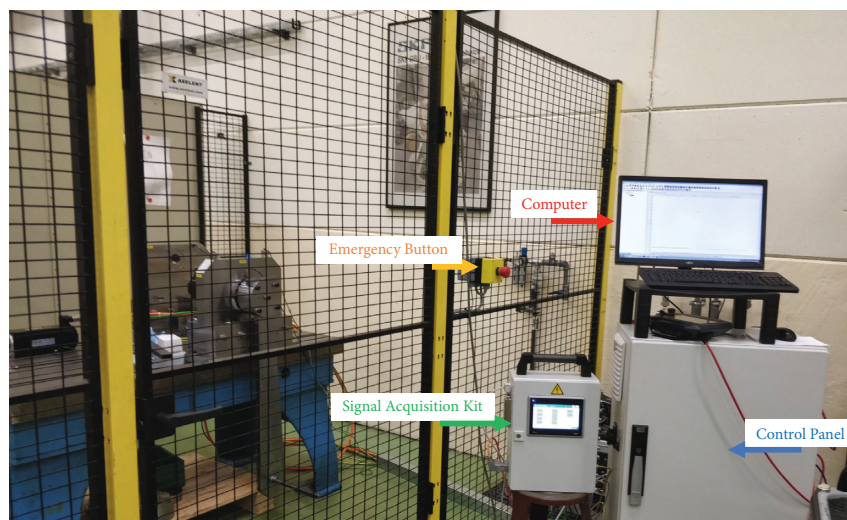


FIGURE 4: Test rig setup.

emergency stop. The mounting of these is of stud mount to allow the minimal sensitivity deviation [29]. The tachometer is placed on the motor side where reflective tape has been

glued to the shaft to allow the correct operation. All these sensors are directly connected to the signal acquisition kit through a direct cable connection.

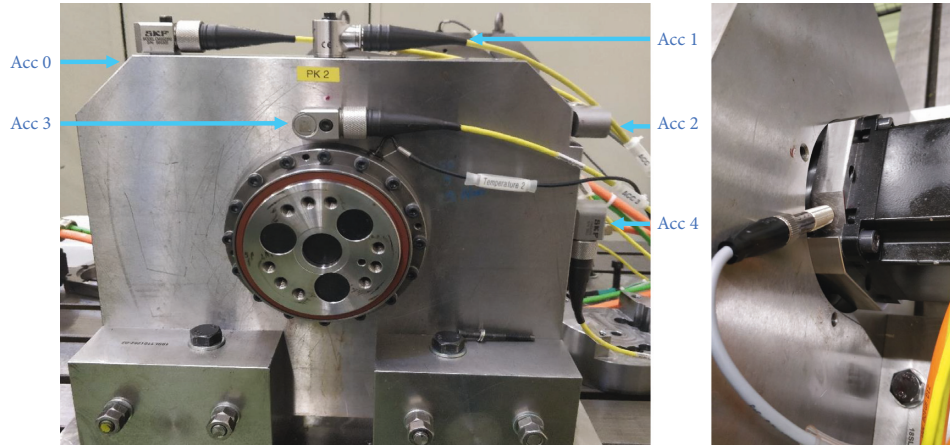


FIGURE 5: Vibration sensors placement. (a) Tachometer placement (b).

TABLE 2: Test rig parameters.

Object	Nomenclature/value
Gearbox	Nabtesco RV-42N
Motor	KEBA KeDrive DMS2-100-0100-60
Weight on arm	30 Kg
Test rig mass	Approximately 2 tons
Accelerometers	5 SKF CMS2200
Tachometer	OBR2500-12GM40-E5-V1

After the description of the sensors' positioning, Figure 6 illustrates the gearbox setup in its initial position (60°) with the noncyclostationary cycle. Cyclostationary in this article represents a constant rotational speed with the angle going from 0 to 180 and back again while noncyclostationary represents variable rotational speed. The gearbox is connected to an arm on which 30 Kg has been added to simulate load. The operating cycle is 3.3 seconds with 3 seconds of rest time to avoid overheating during which the arm performs partial rotations (seen in blue). The combination of the added weight and the chosen cycle is within the operational limits of the chosen gearbox, the Nabtesco RV-42N.

Figures 4–6 describe the test rig setup along with the gearbox setup used in this experiment. The overall parameters are listed in Table 2, indicating the type of sensors, components, and overall weight.

3. Kinematic Study and Signal Processing

This section studies the internal motion of the gearbox indicating each element's frequency and fault frequency and presenting general threshold. The signal processing methods used for the vibrational data are also discussed. The information provided in this section along with Section 2 provides adequate basis to go into the results and discussion section.

3.1. Kinematic Study. The knowledge of the parameters listed in Table 1 and Figure 1 allows the calculation of the overall reduction ratio of the gearbox. In addition to this

ratio (#1), the torque and rotational velocity of each element is shown in Figure 7 with reference to Figure 1. The calculations are done using the Willis equation also known as the fundamental equation of planetary gears with Figure 7 expressing the method described by Muller [30]. The considered gearbox is treated as a typical 2-stage planetary reduction gearbox, where the torque amplification and speed reduction is calculated throughout the present components leading to the overall reduction ratio of 126.

$$i = 1 + Z_2 * \frac{Z_4}{Z_3} = 126. \quad (1)$$

The speed calculations of Figure 7 are done with an input speed of 126 rpm and input torque of 3 Nm with no regard to losses. Each reduction ratio is denoted by i and represents the rotation relation between the input and output component. The first reduction stage is between the input gear and the spur gear. The excentre has the same rotational velocity as the spur gear and the second reduction stage occurs between the RV gear and the Hollow. The RV gear has the same rotational velocity as the Carrier. The overall reduction ratio of 126 represents an ideal output torque of 378 Nm and output speed of 1 rpm. These reduction ratios are used for the frequency calculations of gears and bearings in Section 3.2.

3.2. Frequency Calculations. The usage of the vibration signals and the signal processing techniques allows the detection and visualization of the frequencies, which are either fundamental or fault frequencies. The fundamental frequencies are related to the operation of the gearbox, such as the meshing of the gears. The fault frequencies correspond to the presence of damage or improper operation of the gearbox. The two types of frequencies are described and reported respectively in the upcoming Sections 3.2.1 and 3.2.2 moving into amplitude thresholds in Section 3.2.3. The relative frequencies are reported with reference to the input rotational speed denoted by the input frequency to the system or x as multiples of occurrences during one full rotation of the input shaft.

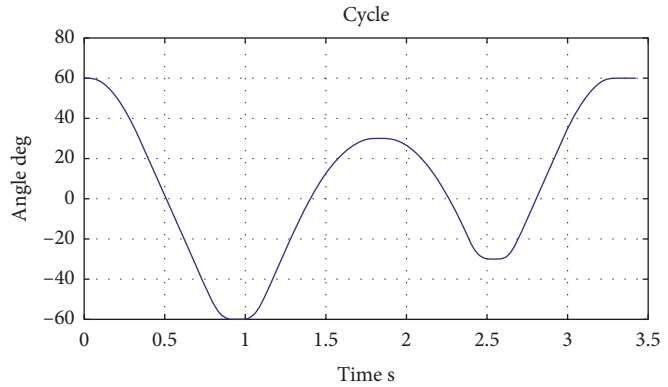
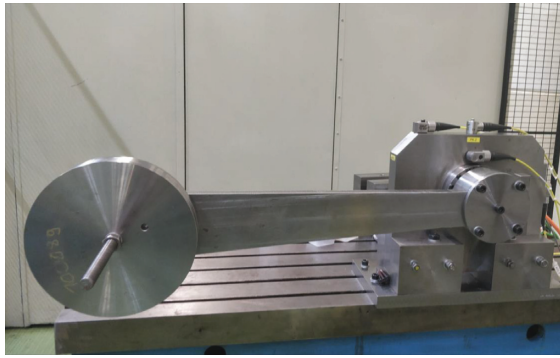


FIGURE 6: Gearbox setup (a). Operating cycle (b).

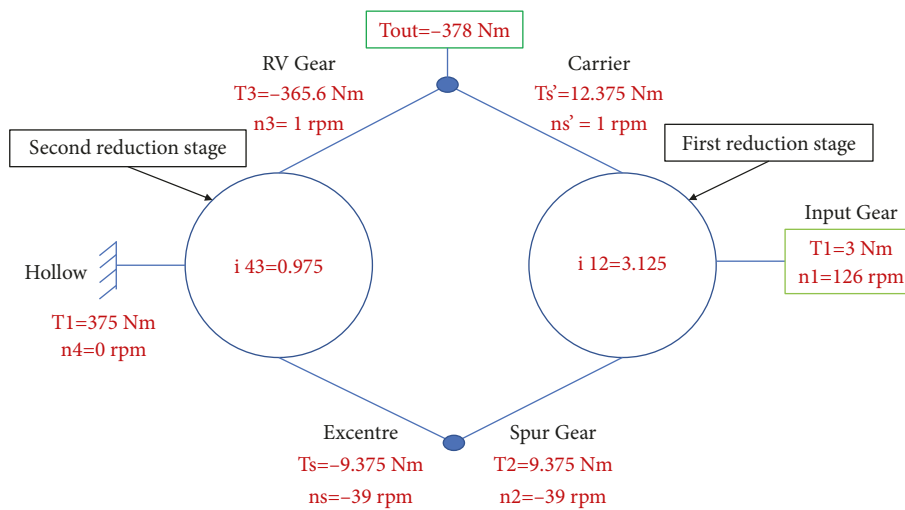


FIGURE 7: Willis equation for torque and velocity calculation on Nabtesco RV-42N.

3.2.1. *Fundamental Frequencies.* The fundamental frequencies result from the operation of the gearbox components and can be divided in this case to the gear meshing and the input speed. The gearbox has 2 reduction stages and as such will have 2 meshing frequencies. The first is called Gear Mesh Frequency (GMF) and the second is Disk Mesh Frequency (DMF) in addition to the input speed (f_i).

Due to the cyclical motion, the notations of the frequencies will be in values of x , which refers to f_i . To simplify, it can be thought as the number of repetitions occurring during one full rotation of the input shaft. The fundamental frequencies are calculated as follows.

$$GMF = Z_1 * f_i = 16 * x,$$

$$DMF = \frac{Z_3}{i} * f_i = 0.309 * x, \quad (2)$$

$$f_i = x.$$

The detection of these frequencies is not only seen as singularities in the frequency domain, but rather they might show up as harmonics or sidebands as shown in Figure 8.

VIBRATION SEVERITY PER ISO 10816					
Machine		Class I small machines	Class II medium machines	Class III large rigid foundation	Class IV large soft foundation
Vibration Velocity V_{rms}	in/s	mm/s			
	0.01	0.28			
	0.02	0.45			
	0.03	0.71			
	0.04	1.12		good	
	0.07	1.80			
	0.11	2.80		satisfactory	
	0.18	4.50			
	0.28	7.10		unsatisfactory	
	0.44	11.2			
	0.70	18.0			
0.71	28.0		unacceptable		
1.10	45.0				

FIGURE 8: Frequency spectrum of a single-stage gearbox without noise.

After the calculation of the fundamental frequencies, the following section discusses the fault frequencies which are either a result from damage or improper operation.

3.2.2. Fault Frequencies. The fault frequencies represent damages of the gearbox, which can show as a new frequency or modulation of the existing fundamental frequencies. The presence of misalignment between the motor and the gearbox is seen as a high amplitude of x , measured axially, in case it is radial and $2x$, measured radially, if it is axial. Wear of the gearbox is observed by higher amplitude of the meshing frequencies and their sidebands. Looseness inside the gearbox is noticed as higher amplitude of the meshing frequencies and half harmonics. These are some of the modulations gearbox damages can make.

Regarding bearing damages, they are seen as a rise of new frequencies regarding the specific damage made. The equations used for the identification of these damages are listed in Appendix A and are calculated after the knowledge of each element's rotational velocity. The ACBB, TRB, and CRB damages, if present, can be directly correlated to their respective fault frequencies. The repetition frequencies of possible defects on a bearing element are reported in Table 3 in orders of frequency.

The damages reported in Figure 3 are three and correlate to 3 modifications in the frequency domain. The first is the ACBB outer ring that correlates to $0.135 * x$ with the second damage correlating to $1.88 * x$, which is the CRB outer ring. The third is the disk damage that should see an increase of the DMF-related frequencies.

3.2.3. Frequency Thresholds. The frequencies discussed in Section 3.2.2 should be visible and propagate to the sensors regarding normal operations of a bearing. In normal bearing monitoring operations, the sensor is set closely to the bearing in operation, which allows the recording of the vibrations. The estimation of the damage or health of the bearing is done from the knowledge of the application, the bearing, and the amplitude of the vibration signals present. Those estimations are made based on experience built from previous recorded experiments done to understand and infer the state of bearings from the amplitudes seen. A more general estimation based on vibration velocity, from the ISO 10816 [31], is shown in the figure below used to infer the state of the asset monitored.

In our work, as shown in Section 2, the bearings are part of the 2-stage reduction gearbox which alters the pure amplitude of the vibration signals of the bearing frequencies as shown in Section 3.3.1. The work presented focuses on identifying the transmitted internal frequencies of the gearbox to infer normal operations or the presence of a defect. The estimation of the defect with the recorded amplitude could be part of a future work that is discussed in Section 4. After the acknowledgements of all the vibration frequencies of the gearbox regarding normal operation and in the presence of damages, the following section describes the signal processing used before discussing the results.

3.3. Signal Processing. This section provides the methods used in the acquired signals in order to infer the state of the gearbox. This first section provides a brief introduction regarding the signals, their path, some signal processing

TABLE 3: Bearings' defect frequencies.

Defect location	Repetition frequency
ACBB inner ring	$0.15 * x$
ACBB outer ring	$0.135 * x$
ACBB rolling element	$0.11 * x$
CRB inner ring	$2.56 * x$
CRB outer ring	$1.88 * x$
CRB rolling element	$2.01 * x$
TRB inner ring	$2.36 * x$
TRB outer ring	$1.76 * x$
TRB rolling element	$1.82 * x$

techniques, and how a gearbox vibration signal would look like. Section 3.3.2 presents briefly Binning and PCA which are, respectively, a signal processing method and a machine learning method with Figure 9 showing a pipeline of them combined.

3.3.1. Traditional Approach. An acquired vibration signal does not represent what is occurring inside the gearbox, but rather the vibrations at that specific sensor position. The reason is that the measured vibrational signal is due to the combination of source effects, internal vibrations, and transmission path effects [32] as shown in Figure 10.

The transmission of the signal from the time domain to the frequency domain is done using the Fast-Fourier Transform (FFT). It offers a very important tool when analyzing signals especially the repetitive type where rather than visualizing peaks in the time domain, they are viewed as a signal amplitude in the frequency domain.

The utilization of FFT is essential; however, a problem rises since it is considered that the sinusoidal signals' cycles are of integer value, but the endpoints are not always continuous. To minimize this effect, a technique called windowing is used, which reduces the amplitude of the discontinuities at the boundaries of each finite sequence acquired by the digitizer [33].

To remove the signals that are not important to the monitored system and to intensify the frequency range where the signals needed to be detected lie in, a method called Enveloping is used. Enveloping used in this work starts with a bandpass filter on the high-frequency signals usually representing the natural frequency of the component in question, after which the signal undergoes some kind of rectifying then a low-pass filter on the low-frequency signals, which can also be an anti-aliasing filter [34]. The modulation that occurs on the signal allows to better detect the source rather than the effect.

Considering noncyclostationary conditions, order tracking is a method to evaluate frequencies as orders where it synchronizes the sampling of input signals to the instantaneous angular position of the machine shaft using a resampling technique. The specific implementation on this setup is done by adjusting the number of samples taken after measuring the speed on each revolution [35]. Rather than a constant number of samples per time, this results in a constant number of samples per revolution and transforms

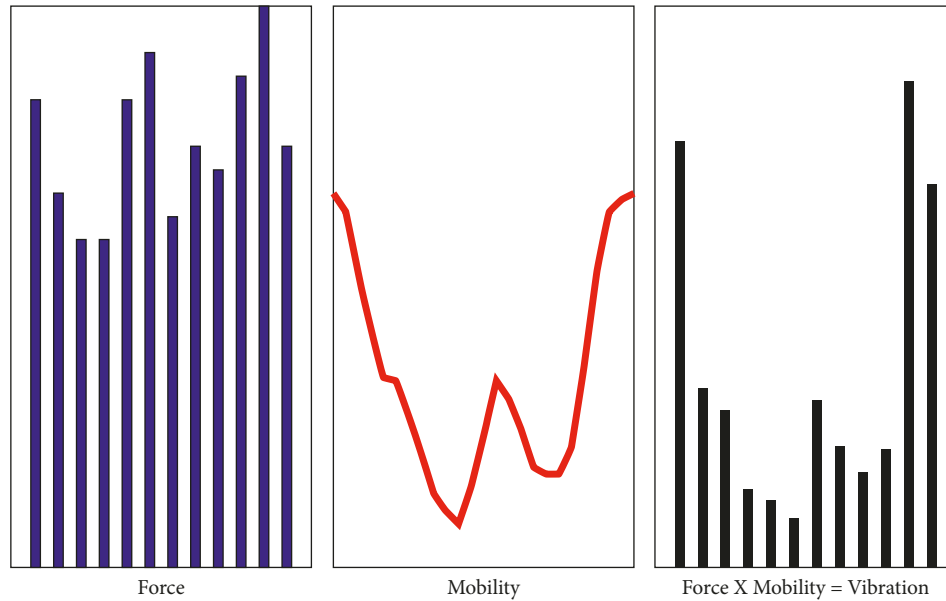


FIGURE 9: Binning and PCA steps.

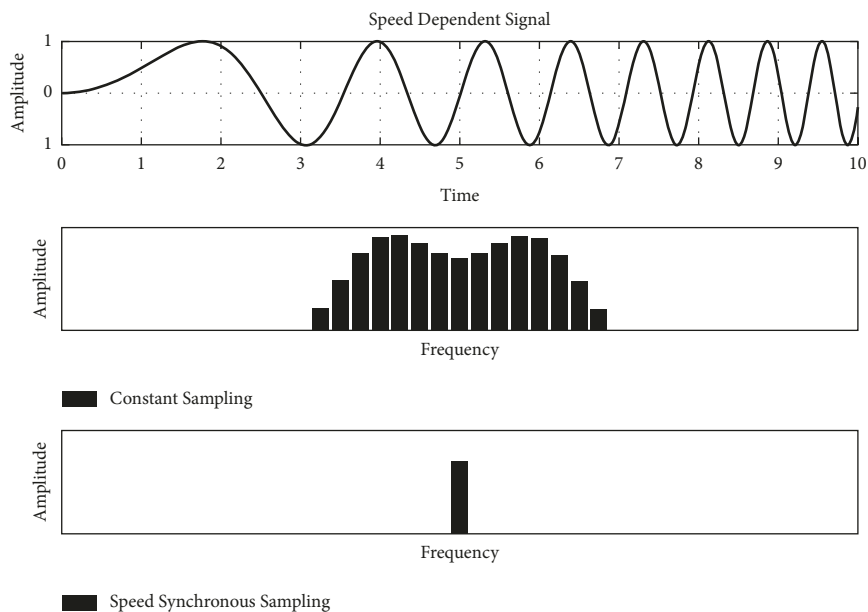


FIGURE 10: Force and transfer path.

the analysis to the order domain rather than the frequency domain. This allows the visualization of frequencies in terms of order rather than Hz avoiding variable speed problems. An example to better explain is found in Figure 11.

In addition to the pure signals, there will also be sidebands and harmonics due to nonlinearities, amplitude modulation, and defects. These modulations to the signals can be also due to a forcing frequency which can then be inferred. Considering a single-stage gearbox with 2 gears, the spectrum will show the input speed, the meshing of the gears as the fundamental frequency with sidebands separated by the input frequency. In addition to that, harmonic signals of the fundamental meshing will be present as seen in Figure 11.

To illustrate the methods used, Figure 12 shows the conditions and steps to obtain the signal visualization required. The techniques used allow various representations where the user can infer the state of the monitored system. In addition, the processing techniques can be altered, with the knowledge of the monitored entity, to achieve better results. The decision to take these steps in the traditional implementation is made in reference to [32] and a recent comprehensive review [36].

3.3.2. Binning and PCA. Binning is a novel SKF developed algorithm used in the context of condition monitoring for partial rotations. It correlates the vibrational signal

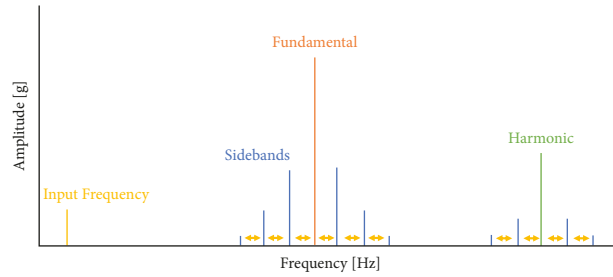


FIGURE 11: Difference in frequency spectrum regarding sampling technique for a speed-varying signal.

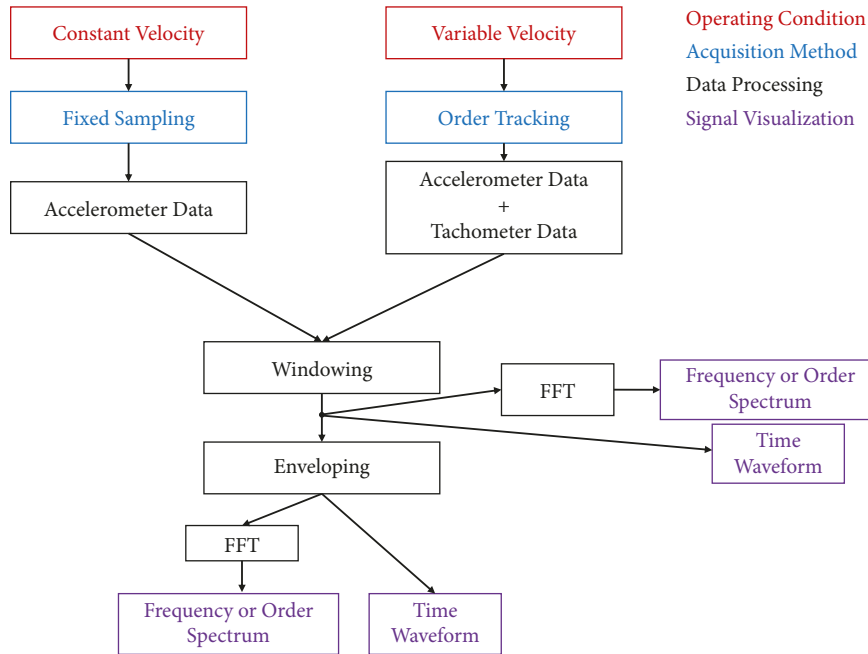


FIGURE 12: Signal processing steps.

extracted from an accelerometer and angular data extracted from an encoder creating angular bins. These angular bins are exploited considering the frequencies that are of interest by choosing bigger or smaller bins. Windowing, filtering, enveloping, and other signal processing techniques are incorporated within and can be used to enhance the results. Then, an FFT is applied after filtering to move into the frequency spectrum. It can be considered as a resampling technique for specific applications. Figure 13 shows the steps in a typical Binning process starting from the acquisition leading to the analysis and the implications. Additional information and full description can be found in the released patent on this invention [37].

PCA, an unsupervised machine learning technique, was invented in 1901 by Karl Pearson [38]. It is usually used as a dimensionality-reduction method where the components aim to reserve the variance of the data. The output is a collection of orthogonal vectors in the direction that best fits the data. The first vector can be defined as a direction with maximum variance of the

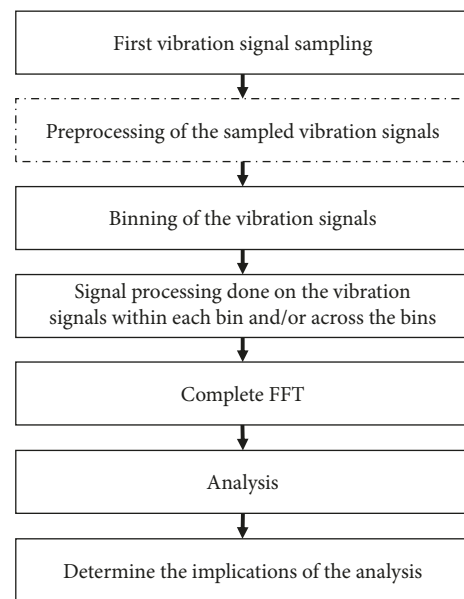


FIGURE 13: Signal processing flow according to the invention.

projected data and the second has less variance but orthogonal to the previous.

The use of Binning in this work is conducted without the data from an encoder but by correlating the angular data from the cycle data that are fed to operate the robotic cycle. The full binning method, as explained in the patent, was not used, but rather partially. The correlation is based upon the start of the cycle observed as an increase in vibration data amplitude, allowing the removal of the key speed sensor, the tachometer. The robotic cycle has a resting phase that corresponds to a period of stop of the motion and low-amplitude vibration signals. The increase in vibration signals' amplitude refers to the start of motion and the predefined cycle of the robot has then be correlated with the vibration data. After this step, FFT is used to go into the order domain. PCA is a second step in the pipeline with the first 2 principal components used for the data projection as Figure 9 shows the steps including Figure 14 and Figure 15.

4. Results and Discussion

The frequencies obtained from the vibration signals after applying the signal processing methods are reported. The results show both the cyclostationary and noncyclostationary conditions. The outcomes show the gearbox with and without the damages; each result is briefly discussed.

Starting with the normal operation of the gearbox, Figure 16 reports the vibration frequencies acquired from the radial accelerometer Acc1 at cyclostationary condition. Figure 17 shows the same frequency domain with less clarity, which is expected when moving into the noncyclostationary conditions.

After the reporting of the vibration signal acquisitions shown in Figures 16 and 17, the clarity and presence of another order, order 8, should be discussed. Regarding the difference in precision between the two figures, it is reported back to the difference in operation and signal acquisition.

At cyclostationary conditions, the speed is constant causing the vibrations to have pure repetitive nature when the signals are acquired. Moving to the noncyclostationary conditions, the velocity acquisition and its correlation to the vibration signals is done using order tracking. The accuracy of the velocity acquired could be the major factor due to the presence of a tachometer and high variations of the velocity in the cycle.

The presence of order 8 and its harmonics could be regarding the presence of 8 poles from the motor side and 16 input teeth (Z1). This combination could be an excitation causing the vibrations to have a measured order 8 in the frequency domain.

An example is shown in Figure 14 where the binning method is used in noncyclostationary conditions. The result resembles that of Figure 17, showing the most dominant frequencies but losing some sharpness in the process. Another factor in this process is the correlation and delay between the vibration signal and the angular data that can be

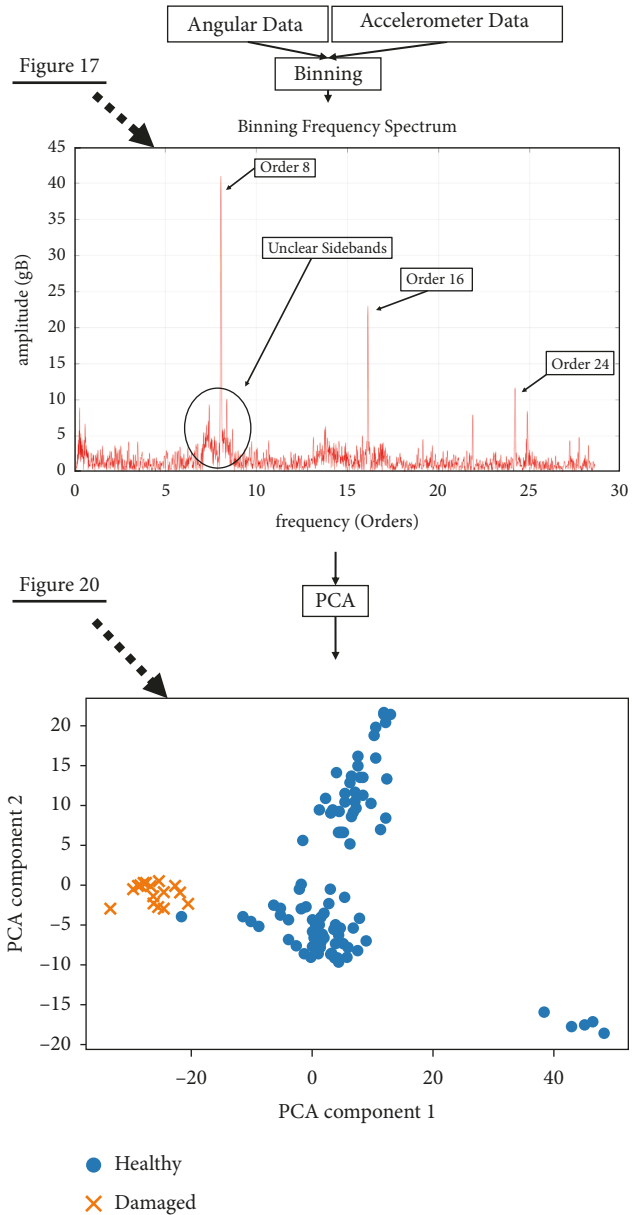


FIGURE 14: Binning noncyclostationary without damage.

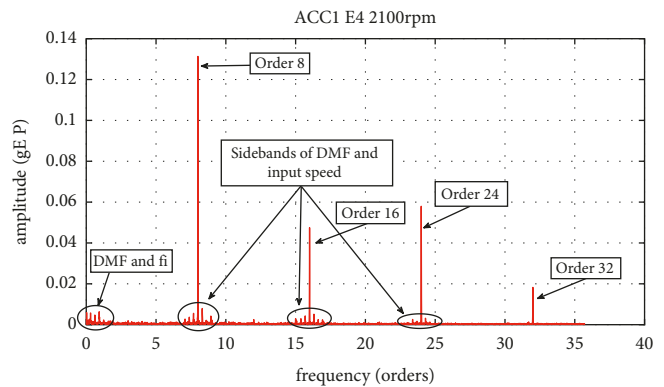


FIGURE 15: PCA components' projection.

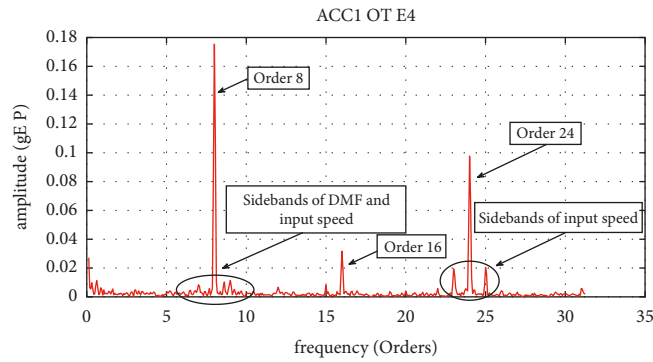


FIGURE 16: Cyclostationary without damage.

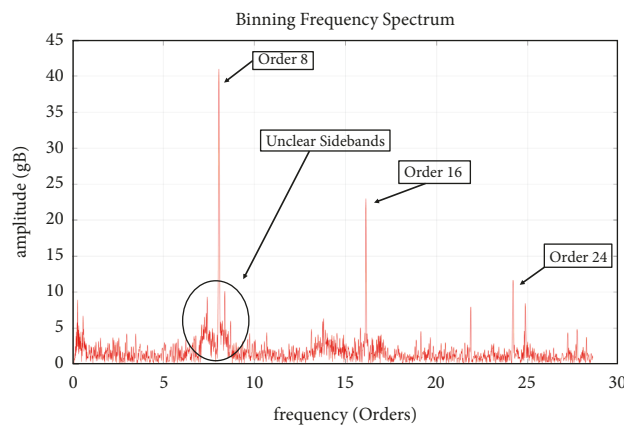


FIGURE 17: Noncyclostationary without damage.

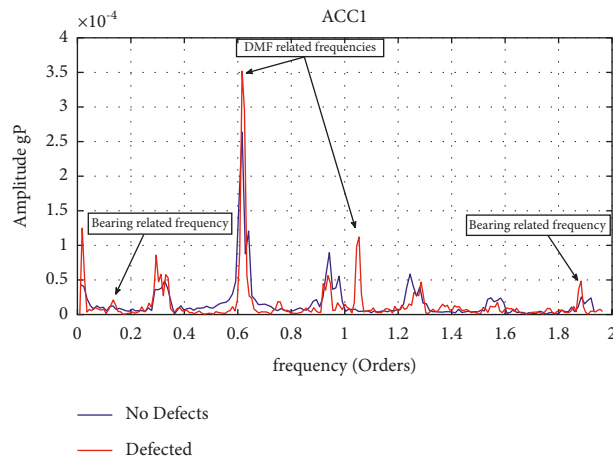


FIGURE 18: Cyclostationary with damage.

improved but the data is still acquired a priori and not actual data from an encoder. In addition, Binning manipulates the amplitude and gB is the amplitude nomenclature chosen.

Regarding the damaged gearbox, the results are reported with a focus on the lower orders of frequencies. The selected damages' frequencies all appear in that field and are reported as before in both cyclostationary and noncyclostationary

conditions. The verification of damages is the rise of 2 new frequencies regarding the bearing damages and increase in vibrations regarding the DMF.

The results shown in Figure 18 and Figure 19 illustrate the vibration frequencies acquired from the radial Accelerometer Acc1 with damage. The figures themselves with the notations clarify the damages and their modulations onto

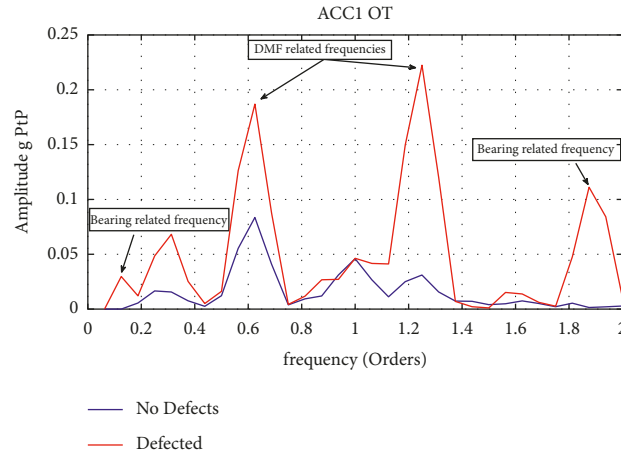


FIGURE 19: Noncyclostationary with damage.

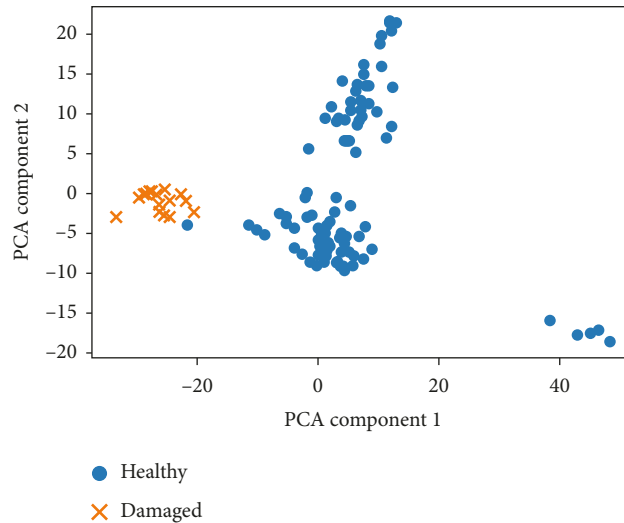


FIGURE 20: Vibration severity per ISO 10816.

TABLE 4: Bearings' variables.

Variables
Number of rolling elements (z)
Diameter of rolling element (dre)
Pitch diameter (dp)
Contact angle (α)
Inner ring rotational velocity ($\dot{\varphi}_{in}$)
Outer ring rotational velocity ($\dot{\varphi}_{out}$)
Inner ring defect repetition frequency (f_{ird})
Outer ring defect repetition frequency (f_{ord})
Rolling element defect repetition frequency (F_{red})

the frequencies. The damages regarding the bearing saw a rise of their respective frequencies and the disk showed an increase of amplitude of its harmonics.

The final process made was using data samples taken from damaged and not damaged gearbox and passed through the Binning and PCA pipeline. 100 samples were acquired for the healthy gearbox and 20 for the damaged. Figure 15 presents the results and it can be seen that some

samples are clustered with each other. All the damaged samples are close to each other with 1 healthy sample near that cluster.

The results shown proved not only the kinematic study of the gearbox but also the ability to detect specific damages within in a nonoptimal laboratory operating conditions. And Figure 17 represents the gearbox in healthy operation using traditional approaches while Figure 14 is done using the Binning algorithm. Figures 18 and 19 show the operation with damage and differences between the two gearbox conditions can be made further than the specified gearbox damages. Figure 15 shows the pipeline result of Binning and PCA that shows the ability to have differences between the two operating conditions.

Section 3.1 provided the kinematic study of the Nabtesco gearbox specifically the RV-42N, but it can also be applied for the other models of the same family. The ability to detect damage in both operating conditions was shown using the defined traditional approach. It is quite an extensive approach and requires knowledge of the asset being monitored and each of its components motion

TABLE 5: Rotation frequencies' equations of the cage and rolling element.

Component	Rotation frequency
Cage	$f_c = \frac{f_{in}}{2}[1 - \frac{dr}{dp} \cos(\alpha)] + \frac{f_{out}}{2}[1 + \frac{dr}{dp} \cos(\alpha)]$
Rolling element	$f_{re} = \frac{dp}{dr} \frac{f_{out} - f_c}{2}[1 + \frac{dr}{dp} \cos(\alpha)]$

TABLE 6: Repetition frequencies of defective location.

Defect location	Repetition frequency
Inner ring	$f_{ird} = z f_c - f_{in} \pm f_{in}$
Outer ring	$f_{ord} = z f_c - f_o \pm f_{out}$
Rolling element	$f_{red} = 2f_{re} \pm f_c$

The presence of \pm is to signify the sidebands of each repetition frequency.

but offers the insight for the elements defect frequencies. The viability of the Binning method, which is tachometer free, showed resemblance to the methods with the tachometer and can be further improved. The combination of Binning and PCA to infer the state of the gearbox was demonstrated in Figure 15 as a nondomain knowledge procedure.

Regarding the work done, improvements regarding the equipment used can be done as in a more accurate tachometer. The stability of the system and data acquired could be improved by considering the vibrational data for the whole cycle and nonshort windows. Other areas could have been explored and are open for future work in the field as a mapping between damage severity and vibration signal amplitudes. The work presented a separated system that can infer the state of the gearbox and then predict the defect present. A step in this methodology would combine the Binning and PCA as a first step and if the gearbox is damaged, the traditional approach would give the damaged component. The exploitation of the Binning approach or similar methods can be studied especially since it can be done with one less sensor, the tachometer.

Another concept in this area is fault estimation from the vibration signals' amplitude and the threshold estimation. A mapping could be done on this gearbox, from the component-level defects and the operating conditions to the fault estimation. That would require a full investigation and testing for several gearboxes with different operating conditions and damages. The results of which could be used to have an estimate similar to Figure 20 but with more precise defects. Such work is needed for faults thresholds and defect size estimations.

An interesting area to explore is the combination of machine learning methods and domain knowledge where this work can be used as a first step. An automatic pipeline that can infer the state and then predict the defect based on sensor data is an avenue to explore. To aid in this, deep learning methodologies can be used injected with the domain knowledge or a complete data-driven method can be used.

5. Conclusion

According to the author's research, until now there is not yet a commercially available technique that makes it possible to detect defects in robots during their normal working conditions. Knowing that a defect occurs within a robot a long

time before actual failure, this work was done on vibration monitoring of a robotic gearbox in order to test the possibility of defect detection.

The work is done with the kinematic study of a robotic gearbox, Nabtesco RV-42N, to understand the vibration frequencies that it emits during motion and the feasibility of detecting the defective element. This work shows a positive result in vibration monitoring of a robotic gearbox, which could be a first step in further investigations and work. The techniques and equipment used, shown in Sections 2.3 and 3.3.1, are well established and widely available. The non-cyclostationary operation conditions of robots have always been a challenge, but with proper tools, this work has shown the ability to identify the root cause of damage before failure.

Binning, a tachometer-free method based on angular data, was presented and the results resemble those of the traditional approach. Binning was then combined with PCA to infer the state of the gearbox as healthy or damaged, and the results presented show a good separation between the two states. As part of the suggested future work, an automatic machine learning pipeline to infer the state and predict the defect of the asset can be done creating a commercialized solution for defect detection in robots.

Appendix

A

This section provides the necessary equations [39] to calculate the defect frequencies of the bearings. Table 4 provides the necessary variables and their nomenclature required for the calculations.

These variables allow to calculate the rotation frequencies of the components and then of the repetition frequency of the defect location using the equations in Table 5.

Then, the repetition frequency of the specific defect location is calculated using the equations shown in Table 6.

Data Availability

The vibration data used to support the findings of this study cannot be made freely available due to the confidentiality of the work as part of an internal project by SKF Group.

Conflicts of Interest

The authors declare that there are no conflicts of interest regarding the publication of this paper.

Acknowledgments

The authors extend their gratitude to SKF Group for the opportunity provided to carry out the presented work. The

research work was funded as part of a joint project by Politecnico di Torino and SKF Group regarding a Master Thesis done by the corresponding author.

References

- [1] M. S. Kan, A. C. C. Tan, and J. Mathew, "A review on prognostic techniques for non-stationary and non-linear rotating systems," *Mechanical Systems and Signal Processing*, vol. 62-63, pp. 1–20, October 2015.
- [2] J. Lee, F. Wu, W. Zhao, M. Ghaffari, L. Liao, and D. Siegel, "Prognostics and health management design for rotary machinery systems—reviews, methodology and applications," *Mechanical Systems and Signal Processing*, vol. 42, no. 1-2, pp. 314–334, 2014.
- [3] Y. Li, F. Tao, Y. Cheng, X. Zhang, and A. Y. C. Nee, "Complex networks in advanced manufacturing systems," *Journal of Manufacturing Systems*, vol. 43, no. 3, pp. 409–421, 2017.
- [4] Ifr, "International federation of robotics," 2018, <https://ifr.org/ifr-press-releases/news/robot-density-rises-globally>.
- [5] Ifr, "International federation for robotics," 2019, <https://ifr.org/downloads/press2018/Executive%20Summary%20WR%202019%20Industrial%20Robots.pdf>.
- [6] A. G. Starr, R. J. Wynne, and I. Kennedy, "Failure analysis of mature robots in automated production," *Proceedings of the Institution of Mechanical Engineers - Part B: Journal of Engineering Manufacture*, vol. 213, no. 8, pp. 813–824, 1999.
- [7] Y. Kim, J. Park, K. Na, H. Yuan, and B. D. Youn, "Phase-based time domain averaging (PTDA) for fault detection of a gearbox in an industrial robot using vibration signals," *Mechanical Systems and Signal Processing*, vol. 138, 2020.
- [8] E. Khalastchi, M. Kalech, and L. Rokach, "A hybrid approach for improving unsupervised fault detection for robotic systems," *Expert Systems with Applications*, vol. 81, pp. 372–383, 2017.
- [9] A. Wing, K. To, P. Gavil, and D. Liu, "A comprehensive approach to real-time fault diagnosis during automatic grit-blasting operation by autonomous industrial robots," *Robotics and Computer-Integrated Manufacturing*, vol. 49, pp. 13–23, 2018.
- [10] M. A. Costa, B. Wullt, M. Norrlöf, and S. Gunnarsson, "Failure detection in robotic arms using statistical modeling, machine learning and hybrid gradient boosting," *Measurement*, vol. 146, pp. 425–436, 2019.
- [11] V. Mien, K. Hee-Jun, S. Young-Soo, and S. Kyoo-Sik, "A robust fault diagnosis and accommodation scheme for robot manipulators," *International Journal of Control, Automation, and Systems*, vol. 11, no. 2, pp. 377–388, 2013.
- [12] H. Schempf and D. R. Yoerger, "Study of dominant performance characteristics in robot transmissions," *Journal of Mechanical Design*, vol. 115, no. 3, pp. 472–482, 1993.
- [13] X. Chang, B. Tang, Q. Tan, L. Deng, and F. Zhang, "One-dimensional fully decoupled networks for fault diagnosis of planetary gearboxes," *Mechanical Systems and Signal Processing*, 2019.
- [14] N. Barbieri, G. de Sant'Anna Vitor Barbieri, B. M. Martins, L. de Sant'Anna Vitor Barbieri, and K. F. de Lima, "Analysis of automotive gearbox faults using vibration signal," *Mechanical Systems and Signal Processing*, vol. 129, pp. 148–163, 2019.
- [15] D. Fritz Plöger, P. Zech, and S. Rinderknecht, "Vibration signature analysis of commodity planetary gearboxes," *Mechanical Systems and Signal Processing*, vol. 119, pp. 255–262, 2019.
- [16] Y. Guo, L. Zhao, X. Wu, and J. Na, "Vibration separation technique based localized tooth fault detection of planetary gear sets: a tutorial," *Mechanical Systems and Signal Processing*, vol. 129, pp. 130–147, 2019.
- [17] S. Xue and I. Howard, "Torsional vibration signal analysis as a diagnostic tool for planetary gear fault detection," *Mechanical Systems and Signal Processing*, vol. 100, pp. 706–728, 2018.
- [18] Y. Li, K. Ding, G. He, and H. Lin, "Vibration mechanisms of spur gear pair in healthy and fault states," *Mechanical Systems and Signal Processing*, vol. 81, pp. 183–201, 2016.
- [19] S. Guoji, S. McLaughlin, X. Yongcheng, and P. White, "Theoretical and experimental analysis of bispectrum of vibration signals for fault diagnosis of gears," *Mechanical Systems and Signal Processing*, vol. 43, no. 1-2, pp. 76–89, 2014.
- [20] X. Yang, K. Ding, and G. He, "Phenomenon-model-based AM-FM vibration mechanism of faulty spur gear," *Mechanical Systems and Signal Processing*, vol. 134, 2019.
- [21] O. D. Mohammed, M. Rantatalo, J.-O. Aidanpää, and U. Kumar, "Vibration signal analysis for gear fault diagnosis with various crack progression scenarios," *Mechanical Systems and Signal Processing*, vol. 41, no. 1-2, pp. 176–195, 2013.
- [22] S. Xue, I. Howard, C. Wang et al., "The diagnostic analysis of the planet bearing faults using the torsional vibration signal," *Mechanical Systems and Signal Processing*, vol. 134, 2019.
- [23] A. Had and K. Sabri, "A two-stage blind deconvolution strategy for bearing fault vibration signals," *Mechanical Systems and Signal Processing*, vol. 134, 2019.
- [24] B. Dolenc, P. Boškoski, and Đ. Juričić, "Distributed bearing fault diagnosis based on vibration analysis," *Mechanical Systems and Signal Processing*, vol. 66-67, pp. 521–532, 2016.
- [25] L. Barbini, M. Eltabach, A. J. Hillis, and J. L. du Bois, "Amplitude-cyclic frequency decomposition of vibration signals for bearing fault diagnosis based on phase editing," *Mechanical Systems and Signal Processing*, vol. 103, pp. 76–88, 2018.
- [26] X. Zhang, Z. Liu, Q. Miao, and L. Wang, "Bearing fault diagnosis using a whale optimization algorithm-optimized orthogonal matching pursuit with a combined time-frequency atom dictionary," *Mechanical Systems and Signal Processing*, vol. 107, pp. 29–42, 2018.
- [27] Nabtesco, "Nabtesco motion control," p. 24, May 2019, <http://www.nabtescomotioncontrol.com/pdfs/rvn-series.pdf>.
- [28] S. Sheng, "National renewable energy laboratory," <https://www.nrel.gov/docs/fy14osti/60982.pdf>.
- [29] S. Shokrollahi, H. Ahmadian, and F. Adel, "An investigation into the accelerometer mounting effects on signal transmissibility in modal measurements," *Scientica Iranica*, vol. 24, no. 5, pp. 2433–2444, 2017.
- [30] H. W. Muller, *Die Umlaufgetriebe*, Springer, Berlin, 1997.
- [31] I. 1 2, "ISO 10816-1:1995," <https://www.iso.org/standard/18866.html>.
- [32] R. B. Randall, *Vibration Based Condition Monitoring*, Wiley, West Sussex, 2011.
- [33] N. instruments, 2019, <http://download.ni.com/evaluation/pxi/Understanding%20FFTs%20and%20Windowing.pdf>.
- [34] X. Liang, M. J. Zuo, and L. Liu, "A windowing and mapping strategy for gear tooth fault detection of a planetary gearbox," *Mechanical Systems and Signal Processing*, vol. 80, pp. 445–459, 2016.
- [35] S. Group, *@ptitude Observer 10.2, Revision N*, SKF Condition Monitoring Center, Luleå, 2017.

- [36] W. R. Mohamad Hazwan Mohd Ghazali, "Vibration analysis for machine monitoring and diagnosis: a systematic review," *Shock and Vibration*, vol. 2021, p. 25, 2021.
- [37] A. Thomson and V. S. United, *States of America Patent*, vol. 10, no. 914, p. 656, 2021.
- [38] K. Pearson, "LIII. On lines and planes of closest fit to systems of points in space," *The London, Edinburgh, and Dublin Philosophical Magazine and Journal of Science*, vol. 2, no. 11, pp. 559–572, 1901.
- [39] G. Van Nijen, P. Van Dalen, G. Angelov Dimitrov et al., *Noise and Vibration in Bearing Systems*, SKF Research & Technology Development, 2 edition, 2017.